

Chaotic Compressed Sensing for Secure Image Transmission in LoRa IoT Systems

Chatchai Wannaboon¹, Shamsul Ammry Bin Shamsul Ridzwan², Sorawit Fong-In^{3*}

Intelligent Electronics System Laboratory,

Thai-Nichi Institute of Technology, Bangkok, Thailand 10250^{1,3}

School of Engineering, Temasek Polytechnic, Singapore 529757²

Abstract—Transmitting image data reliably over long distances with low cost and minimal storage consumption is critical for LoRa-enabled IoT devices. Conventional methods often rely on high-power consumption or computationally intensive hardware, rendering them unsuitable for cost-sensitive and resource-limited IoT deployments. This paper presents a hybrid compressed sensing approach designed for efficient image transmission in LoRa-based IoT systems. The proposed method utilizes a chaotic map-based sensing matrix to enhance randomness and incoherence in the sampling process, which also serves as an encryption key to secure the transmitted data. While wavelet transform is combined with Total Variation (TV) minimization to accurately recover high-quality images from the sparse measurements on the reconstruction side. The system is implemented on low-power development boards, with the ESP32-CAM used for image capture and initial compression, and the CubeCell-AB01 handling LoRa-based wireless transmission. Experimental results demonstrate significant reductions in data size and transmission cost, while preserving image fidelity and enhancing data security, making the proposed method well-suited for resource-constrained IoT applications.

Keywords—Secure image transmission; compressed sensing; chaotic maps; long-range radio signals; LoRa

I. INTRODUCTION

The rapid growth of the Internet of Things (IoT) has led to the widespread deployment of low-power embedded devices in various fields, including smart agriculture, environmental monitoring, industrial automation, and remote surveillance. These applications require the transmission of image data from edge devices to centralized servers or cloud platforms for real-time analysis and decision-making. However, transmitting image data over constrained wireless communication protocols remains a major challenge. One of the most promising technologies for long-range, low-power wireless communication is LoRa (Long Range), which operates in the sub-GHz ISM band and enables communication over distances of several kilometers while consuming minimal energy. LoRa is a core component of LoRaWAN, a Low Power Wide Area Network (LPWAN) protocol that supports battery-operated devices with low data rates and long-range connectivity [1], [2], [3]. Despite its benefits, LoRa's limited bandwidth makes it unsuitable for direct transmission of large multimedia data such as images without significant pre-processing or compression. This limitation highlights the need for innovative methods that can enable efficient and secure image transmission over LoRa networks, particularly in resource-constrained IoT environments.

To address this, researchers have combined LoRa with data reduction strategies. For example, [4], [5] used downsampling and lightweight encoding for transmitting grayscale images over LoRa. However, such approaches often compromise image quality or fail to address security concerns.

Image compression and transmission techniques are often require intensive computation or large memory storage, both of which are impractical for resource-constrained IoT devices. Moreover, ensuring the security and privacy of image data during wireless transmission is becoming increasingly important, particularly in applications involving sensitive or personal information [6], [7], [8]. Conventional compression algorithms such as JPEG and JPEG2000 are widely used in standard multimedia systems but are not well-suited for resource-constrained IoT devices. These methods often require substantial computational resources for encoding and decoding, as well as a significant memory footprint for storing compressed images. Such a study has proposed by [9], [10], [11] highlights the limitations of traditional algorithms like JPEG in IoT scenarios, particularly under power and bandwidth constraints. Moreover, such methods typically do not address data privacy or encryption, leaving image data vulnerable to interception during wireless transmission.

Recently, compressed sensing (CS) has emerged as a promising alternative for image acquisition and transmission in IoT systems [12], [13], [14]. CS enables signal recovery from a small set of linear, provided the original signal is sparse in some domain. Its application to image data allows significant reductions in the number of transmitted samples, thereby saving bandwidth and energy. In [15], the authors demonstrated the effectiveness of CS for single-pixel imaging, laying the groundwork for its use in bandwidth-limited environments. In addition, [16] applied Total Variation (TV) minimization and wavelet transforms to enhance image reconstruction quality from sparse measurements. In [17], [18], CS offers significant advantages for improving data acquisition and transmission efficiency. By leveraging sparse representation and reconstruction algorithms, CS bypasses the constraints of the Shannon-Nyquist sampling theorem, enabling accurate signal recovery from a reduced number of measurements. This approach supports energy-efficient processing and reduces bandwidth requirements, making it particularly suitable for applications with limited communication resources. Consequently, CS is a promising solution to address the challenges of data transmission and storage in resource-limited environments.

The use of chaotic maps to generate sensing matrices has gained popularity due to their inherent randomness, un-

*Corresponding authors.

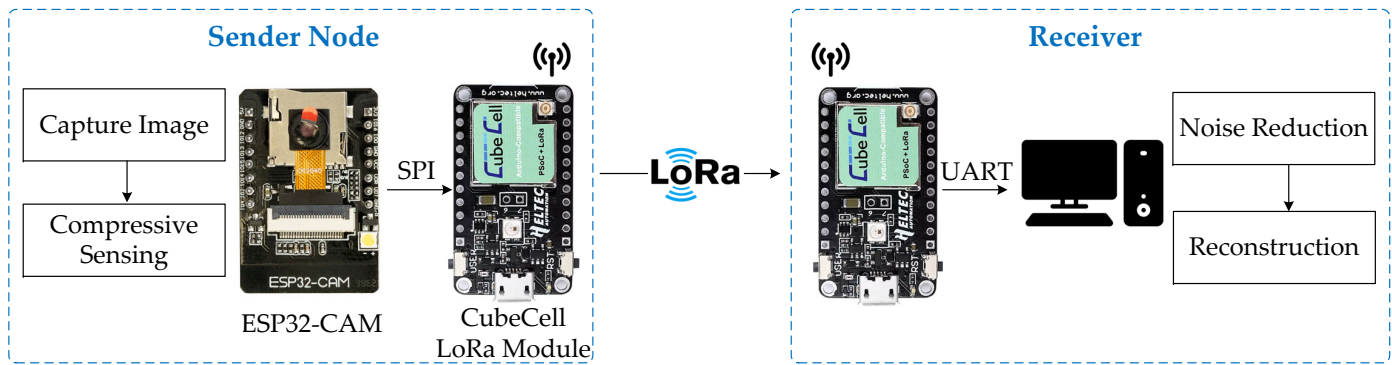


Fig. 1. Overview of the proposed system.

predictability, and suitability for lightweight encryption [19]. Chaotic systems, such as the Logistic or Tent maps, have been shown to produce pseudo-random sequences with high sensitivity to initial conditions, making them ideal for both compressed sampling and security [20]. In [21], a chaotic sensing matrix was integrated into CS to achieve both efficient sampling and data confidentiality. Such dual-purpose matrices reduce the need for separate encryption steps, thereby saving computational resources in IoT applications. Recent work in [22] explores advancements in Compressed Sensing (CS) within the context of emerging IoT technologies. Among the various sensing techniques discussed, Chaotic Compressed Sensing stands out for its effectiveness in enhancing image security and improving randomness in the sampling process. While this approach offers advantages in both data protection and acquisition efficiency, the quality of image reconstruction remains highly dependent on the use of suitable recovery algorithms. Even minor variations in system parameters or the presence of environmental noise can significantly degrade reconstruction accuracy, highlighting the sensitivity and complexity of the process. The paper is organized as follows: Section II provides the equipments and data collection; Section III describes the proposed model architecture and its components in detail; Section IV presents experimental results and comparative analysis; and Section V concludes the paper with a summary of findings.

Therefore, this paper presents a hybrid compressed sensing framework that combines chaotic map-based sensing with advanced reconstruction techniques. The proposed approach leverages the inherent randomness and sensitivity of chaotic systems not only to improve measurement incoherence but also to embed encryption at the acquisition stage, ensuring data security. The reconstruction process employs a combination of wavelet transform and Total Variation (TV) minimization, enabling accurate image recovery from a limited number of compressed measurements. This framework is implemented and validated on resource-constrained development boards, demonstrating its practicality for real-world IoT deployments. By integrating efficiency, robustness, and security, the proposed method provides a comprehensive solution for image transmission in bandwidth-limited and energy-constrained IoT environments.

II. SYSTEM OVERVIEW

The proposed system is designed to enable efficient and secure image transmission over LoRa-based IoT networks by integrating a hybrid compressed sensing framework that leverages chaotic maps and advanced image reconstruction techniques. The architecture consists of two main components: an edge device responsible for image acquisition and compression, and a LoRa node for wireless transmission to a receiver. The overview of the proposed system is shown in Fig. 1. An ESP32-CAM module is used to capture images from the environment. Due to the limited computational resources of the device, traditional image compression techniques are unsuitable. Instead, the system applies Compressed Sensing (CS) using a chaotic map-generated sensing matrix, which not only reduces the number of measurements needed for transmission but also introduces inherent randomness that functions as a lightweight encryption mechanism. This dual-purpose matrix allows secure and compressed data acquisition with minimal processing overhead. Once the image has been compressed into sparse measurements, the data is transmitted from the ESP32-CAM to a LoRa node (CubeCell-AB01) via Serial Peripheral Interface (SPI), a high-speed, full-duplex communication protocol suitable for real-time microcontroller interconnection. The CubeCell-AB01, equipped with an SX1276 LoRa transceiver, then transmits the compressed and encrypted measurements wirelessly over long distances using the LoRa modulation scheme, which is ideal for low-power and low-bandwidth applications.

On the receiving side, the data is collected and processed using a reconstruction algorithm that combines wavelet transform with Total Variation (TV) minimization. The wavelet transform provides a sparse representation of the original image, while TV minimization enhances the quality of reconstruction by preserving edge information and reducing noise artifacts. The reconstruction process is executed on a computational node with sufficient resources, such as a laptop or a cloud server, to restore the image with high fidelity from the limited number of compressed samples. This architecture is specifically designed to operate under the constraints of IoT environments, offering a balance between transmission efficiency, energy consumption, and image quality. The integration of chaotic sensing and hybrid reconstruction ensures that the system not only minimizes the amount of data transmitted but also maintains privacy and robustness against channel noise.

Algorithm 1: Image Sampling with Chaotic Compressed Sensing

Input: Grayscale image I of size (H, W) (8-bit)
Input: Chaotic control parameter r , initial value X_0 , threshold $\in [0, 1]$
Output: Array y_{nonzero} of (index, value) pairs

```
1  $x \leftarrow \text{reshape}(I, N)$ ,  $N \leftarrow H \times W$ ;  
2  $X \leftarrow X_0$ ;  
3 for  $i \leftarrow 1$  to  $N$  do  
4    $X \leftarrow X/|X| - r \cdot X$ ; // Signum chaotic  
   map  
5    $\text{chaotic\_seq}[i] \leftarrow X$ ;  
6 end  
7 Normalize  $\text{chaotic\_seq}$  to range  $[0, 1]$ ;  
8 for  $i \leftarrow 1$  to  $N$  do  
9   if  $\text{chaotic\_seq}[i] > \text{threshold}$  then  
10     $\text{mask}[i] \leftarrow 1$ ;  
11  else  
12     $\text{mask}[i] \leftarrow 0$ ;  
13  end  
14 end  
15 for  $i \leftarrow 1$  to  $N$  do  
16    $y[i] \leftarrow \text{mask}[i] \cdot x[i]$ ;  
17 end  
18  $y_{\text{nonzero}} \leftarrow \emptyset$ ;  
19 for  $i \leftarrow 1$  to  $N$  do  
20   if  $y[i] \neq 0$  then  
21     Append  $(i, y[i])$  to  $y_{\text{nonzero}}$ ;  
22   end  
23 end  
24 Transmit  $y_{\text{nonzero}}$  over SPI to LoRa transmitter;
```

A. Chaotic-Based Sensing Matrix Generation

The compressed sensing process relies on a pseudo-random measurement matrix that satisfies the Restricted Isometry Property (RIP) and ensures incoherence with the sparsifying basis. In order to meet these requirements while also provide lightweight encryption, this work employs a chaotic map-based approach to generate the sensing matrix. The signum chaotic map, which is sensitivity to initial conditions and ability to generate highly random-like sequences from deterministic equations [23], [24], is given by:

$$X_{n+1} = \text{sign}(X_n) - rX_n \quad (1)$$

where r is a chaos tuning parameter. The simple form of (1) can be considered by

$$X_{n+1} = \frac{X_n}{|X_n|} - rX_n \quad (2)$$

where, X_n is the state at iteration n , and r , is the control parameter that determines the chaotic behavior. For appropriate values of r , the system exhibits aperiodic, non-converging sequences, making it suitable for generating random measurement matrices with strong incoherence properties. The measurement matrix generation can be achieved, following this procedure:

Algorithm 2: Image Reconstruction

Input: Compressed data y_{nonzero} (index, value pairs), image size (H, W) , chaotic map parameters r , X_0 , threshold, initial threshold λ , decay factor λ_{decay} , number of iterations
Output: Reconstructed image x_{recon} of size (H, W)

```
1  $N \leftarrow H \times W$ ;  
2 Initialize  $x_{\text{full}}$  as a zero vector of length  $N$ ;  
3 for  $(i, \text{val}) \in y_{\text{nonzero}}$  do  
4    $x_{\text{full}}[i] \leftarrow \text{val}$ ;  
5 end  
6  $y_{\text{reshaped}} \leftarrow \text{reshape}(x_{\text{full}}, H, W)$ ;  
7 Step 1: Regenerate chaotic binary mask;  
8  $X \leftarrow X_0$ ;  
9 for  $i \leftarrow 1$  to  $N$  do  
10    $X \leftarrow X/|X| - r \cdot X$ ; // Signum chaotic  
   map  
11    $\text{chaotic\_seq}[i] \leftarrow X$ ;  
12 end  
13 Normalize  $\text{chaotic\_seq}$  to range  $[0, 1]$ ;  
14 for  $i \leftarrow 1$  to  $N$  do  
15   if  $\text{chaotic\_seq}[i] > \text{threshold}$  then  
16      $\text{mask}[i] \leftarrow 1$ ;  
17   else  
18      $\text{mask}[i] \leftarrow 0$ ;  
19   end  
20 end  
21  $\text{mask} \leftarrow \text{reshape}(\text{mask}, H, W)$ ;  
22 Step 2: Iterative reconstruction;  
23  $x_{\text{hat}} \leftarrow y_{\text{reshaped}}$ ;  
24 for  $i \leftarrow 1$  to  $\text{iterations}$  do  
25    $(\text{flat}, \text{slices}) \leftarrow \text{WaveletTransform}(x_{\text{hat}})$ ;  
26    $\text{flat\_thresh} \leftarrow \text{SoftThreshold}(\text{flat}, \lambda)$ ;  
27    $x_{\text{hat}} \leftarrow$   
   InverseWaveletTransform( $\text{flat\_thresh}$ ,  $\text{slices}$ );  
28   for  $\text{pixel } (m, n)$  do  
29     if  $\text{mask}[m, n] = 1$  then  
30        $x_{\text{hat}}[m, n] \leftarrow y_{\text{reshaped}}[m, n]$ ;  
31     end  
32   end  
33    $x_{\text{hat}} \leftarrow \text{TVDenoise}(x_{\text{hat}}, \text{weight} = 0.025)$ ;  
34    $\lambda \leftarrow \lambda \cdot \lambda_{\text{decay}}$ ;  
35 end  
36 Clip values in  $x_{\text{hat}}$  to range  $[0, 1]$ ;  
37 return  $x_{\text{recon}} \leftarrow x_{\text{hat}}$ ;
```

- Select a suitable initial condition $X_0 \in \{-1, 1\}$ and a control parameter $r \in \mathbb{R}$ that ensures chaotic behavior ($X_0 = 0.1$ and $r = 1.99$ in this experiment). Both values can be utilized as secret keys for encryption purposes.
- Iterate the signum chaotic map to generate a 1D chaotic sequence $\{X_n\}$. The total number of iterations should be equal to the number of elements required in the measurement matrix, i.e. $M \times N$, where M is the number of measurements and N is the signal/image dimension after vectorization.
- Normalize the chaotic sequence and optionally apply

binarization (e.g. using sign function) or map it to a standard distribution (e.g. Gaussian or Bernoulli) to match common CS practices.

The use of the signum chaotic map introduces an intrinsic encryption feature, as the sensing matrix depends heavily on the initial value X_0 and parameter r . Any slight variation in these parameters leads to entirely different matrices, making it extremely difficult to reconstruct the original image without the correct key. Thus, the chaotic map not only supports compressed sensing but also secures the data at the acquisition stage without the need for additional encryption layers.



Fig. 2. Custom-designed embedded device of transmission node.

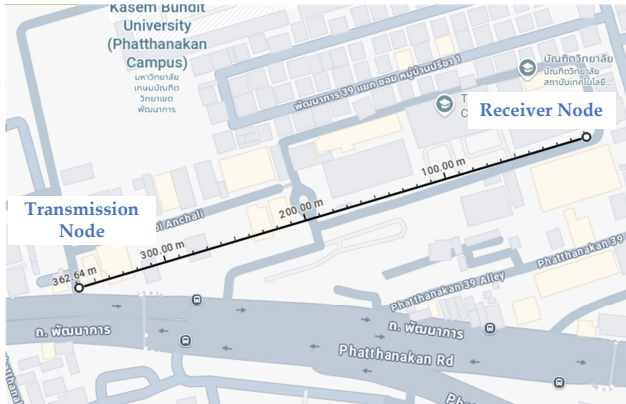


Fig. 3. Testing site of the proposed system.

TABLE I. SUMMARIZE OF LoRa COMMUNICATION PARAMETER

Parameters	Value
LoRa Module	SX1262
Frequency	923 MHz
Spreading Factor	7
Coding Rate	4/5
Transmission Power	14 dBm

B. Image Sampling via Compressed Sensing

The image acquisition process is carried out using the principles of Compressed Sensing (CS), a signal processing technique that enables accurate recovery of sparse or compressible signals from a small number of linear measurements. This is particularly beneficial for image transmission in IoT systems, where bandwidth, memory, and energy are severely constrained. Let $x \in \mathbb{R}^N$ represent the original image signal in vectorized form, e.g. a grayscale image flattened into a 1D array. Under the CS framework, instead of acquiring the full signal x , a reduced number of linear measurements $y \in \mathbb{R}^M$ can be acquired with $M \ll N$ by projecting the signal onto a measurement matrix $\Phi \in \mathbb{R}^{M \times N}$. The data acquisition model can be expressed by:

$$y = \Phi x \quad (3)$$

In order to ensure that x can be reconstructed from y , the signal must be sparse in some transform domain. That is, there exists a sparsifying basis Ψ such that

$$x = \Psi s \quad (4)$$

where, s is a sparse coefficient vector. Substituting into the measurement equation yields:

$$y = \Phi \Psi s = \Theta s \quad (5)$$



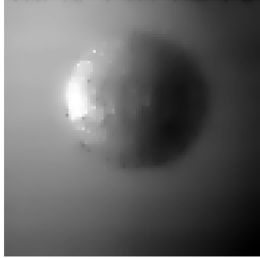
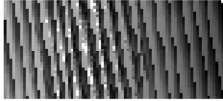
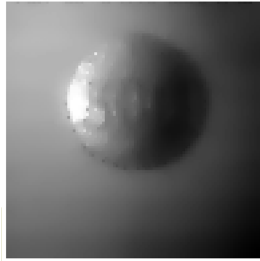
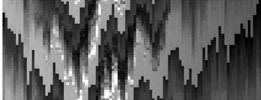
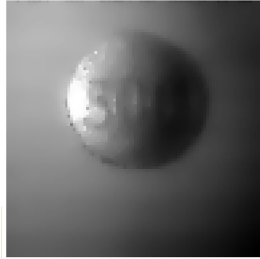
where, $\Theta = \Phi \Psi$ is the effective sensing matrix. The reconstruction of x involves recovering the sparse vector s from y and applying the inverse transform. In the proposed system, the compressed sensing matrix Φ is generated using signum chaotic map (as described in Section 2.1). This chaotic matrix introduces both measurement incoherence and data-level encryption. The image captured by the ESP32-CAM is first converted into grayscale and then vectorized into x . This vector is multiplied by Φ to produce the compressed measurements y , which are significantly smaller in size than the original image.

The sampling process begins with image acquisition from the camera module, followed by preprocessing steps that include grayscale conversion and normalization. The resulting image is then vectorized into a one-dimensional signal x , which is subsequently projected onto a chaotic map-generated sensing matrix Φ to compute the compressed measurements $y = \Phi x$. Finally, the compressed vector y is transmitted via the Serial Peripheral Interface (SPI) to the LoRa transmitter for wireless delivery. The pseudo-code of image acquisition and compressed sensing is illustrated in the Algorithm 1.

C. Reconstruction Algorithm

After compressed measurements are transmitted via LoRa and received by a computational node, the next step is to reconstruct the original image from the sparse measurement vector. The reconstruction process is designed to recover the original image from the received compressed measurements by leveraging the same chaotic sequence used during sampling.

TABLE II. PERFORMANCE EVALUATION OF COMPRESSED AND RECONSTRUCTED IMAGES OVER DIFFERENT COMPRESSION RATIOS

Original Image	CR	Compressed Image	Reconstructed Image	MSE	PSNR (dB)
	0.2			0.159	31.97
	0.3			0.123	32.92
	0.4			0.102	34.03

This approach ensures both spatial consistency and security by deterministically regenerating the sampling pattern.

First, the receiver regenerates the chaotic sequence (2) using the same initial condition and control parameter r as used during the sampling process. This sequence is normalized and binarized with a fixed threshold to reproduce the binary sampling mask, which distinguishes between known (non-zero) and unknown (zero) pixel locations. The received measurements are reshaped into the original image dimensions, and zero values are re-inserted at positions determined by the chaotic mask. This forms a sparse image matrix where only a subset of pixel values is available. The reconstruction process begins with this sparse image as the initial estimate and iteratively refines it using a combination of wavelet-domain sparsity enforcement and total variation (TV) denoising. Next, the reconstruction loop proceeds by transforming the current image estimate \hat{x} into the wavelet domain using a two-dimensional discrete wavelet transform, resulting in a sparse representation of the image coefficients. A soft-thresholding function is then applied to these coefficients to suppress noise and enforce sparsity. This function shrinks coefficients toward zero based on a threshold λ that decays over iterations as follows:

$$\tilde{X} = \text{sign}(X) \cdot \max(|X| - \lambda, 0) \quad (6)$$

where, X and \tilde{X} are the wavelet coefficient and the thresh-

old coefficient, respectively. The threshold coefficients are subsequently transformed back into the spatial domain via the inverse wavelet transform, resulting in an updated image estimate. To ensure consistency with the original measurements, the known pixel values identified using the chaotic mask are reinserted into their respective positions. This operation can be mathematically expressed as:

$$\hat{x}^{(k)}[i] = \begin{cases} y[i], & \text{if } i \in \Omega. \\ \hat{x}^{(k)}[i], & \text{otherwise} \end{cases} \quad (7)$$

where, Ω is the set of known pixel indices from the chaotic sampling mask, and $\hat{x}^{(k)}$ is the reconstructed image at iteration k . To further refine the output, total variation denoising is applied to the reconstructed image to reduce artifacts and preserve edge structures. This can be formulated as the minimization of the TV norm, given by:

$$\min_x ||x||_{TV} \quad \text{subject to} \quad x \approx \tilde{x} \quad (8)$$

This iterative refinement is performed for 350 iterations. The threshold λ is initialized at 0.1 and decayed by a factor of 0.95 after each iteration to gradually enhance image details. Finally, the reconstructed image is clipped to the valid grayscale range $[0, 1]$. This hybrid reconstruction approach effectively balances sparsity promotion, noise suppression, and

data fidelity, allowing high-quality image recovery from highly compressed chaotic measurements. The pseudo-code of image reconstruction process is illustrated in the Algorithm 2.

III. EXPERIMENTAL RESULTS

To validate the effectiveness of the proposed hybrid compressed sensing approach for image transmission over LoRa-based IoT networks, real-world experiments were conducted using ESP32-CAM as the image acquisition and compression node, and CubeCell AB01 as the LoRa communication. Fig. 2 illustrates the custom-designed embedded system used for field deployment of the proposed image transmission framework. These tests aimed to evaluate system performance in practical conditions, including image quality, transmission efficiency, and hardware feasibility in a low-power wireless environment.

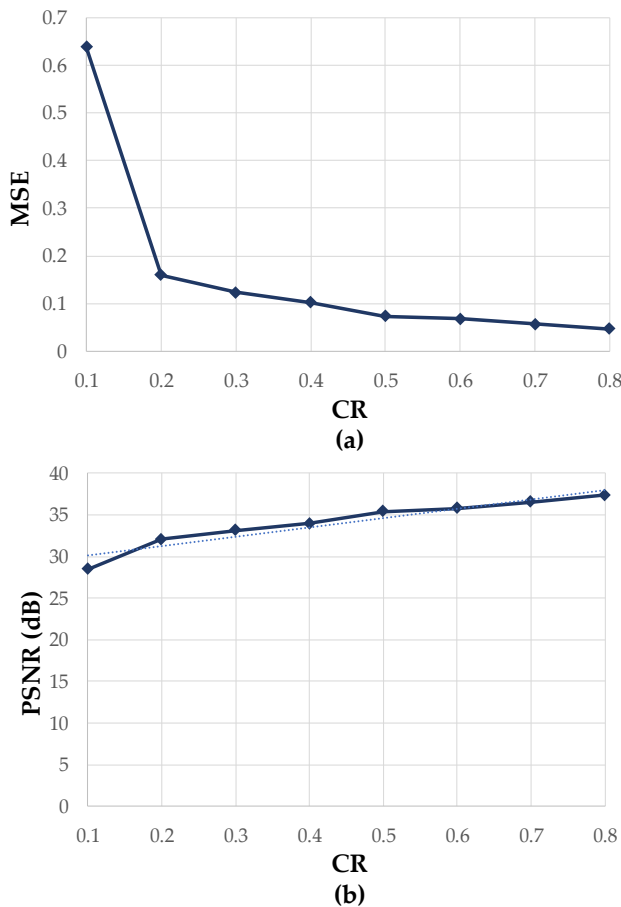


Fig. 4. Compression ratio vs (a) MSE and (b) PSNR.

A. Field Deployment

Fig. 3 shows the real-world testing site of the proposed image transmission system at the Thai-Nichi Institute of Technology (TNI) campus, specifically across the length of the Faculty of Engineering building. The devices were powered by portable USB battery packs and tested over a range of distances (up to 300 meters) with clear line-of-sight. The transmission path included partial obstructions such as walls, corridors, and concrete pillars, making it a meaningful scenario to assess

LoRa signal reliability, data transmission performance, and image reconstruction quality over medium-range distances. Table I summarizes the LoRa parameters in the experiment.

B. Evaluation Metrics

This paper selects Mean Squared Error (MSE) as the primary loss function for training the reconstruction model. It measures the average squared difference between the reconstructed image and the original image, defined mathematically as:

$$\text{MSE} = \frac{1}{N} \sum_{i=1}^N [y_i - f(x_i)]^2 \quad (9)$$

where, N represents the total number of image pixels (or samples), y_i is the ground truth pixel value, and $f(x_i)$ is the predicted pixel value. MSE serves as a direct indicator of reconstruction accuracy. Otherwise, the lower of MSE indicates the closer the reconstructed image is to the original.

To further assess the quality of the reconstructed images, Peak Signal-to-Noise Ratio (PSNR) is employed as quantitative evaluation metrics. PSNR is a widely used objective metric in image processing that reflects the ratio between the maximum possible pixel value and the magnitude of the reconstruction error, and is expressed in decibels (dB). It is calculated as:

$$\text{PSNR} = 10 \cdot \log_{10} \left(\frac{M^2}{\text{MSE}} \right) \quad (10)$$

where, M is the maximum possible pixel intensity value of the image. A higher PSNR indicates better reconstruction quality and lower image distortion, e.g. a PSNR value above 30 dB generally suggests that the reconstructed image is of good visual quality.

C. Performance Analysis

Table II presents a visual and quantitative analysis of the proposed reconstruction system under varying compression ratios (CR) of 0.2, 0.3, and 0.4. The original image is shown in the first column. The second column shows the encrypted or compressed image as produced by chaotic compressed sensing, appearing as random patterns with no visual resemblance to the original. The third column displays the reconstructed images after applying the wavelet-based soft-thresholding and total variation (TV) denoising algorithm. As the CR increases from 0.2 to 0.4, the quality of the reconstructed image significantly improves. This is further supported by the quantitative metrics in MSE and PSNR. At CR = 0.2, the MSE is 0.159 with a PSNR of 31.97 dB, while at CR = 0.4, the MSE reduces to 0.102 and the PSNR increases to 34.03 dB. These results confirm that higher compression ratios yield more accurate image reconstruction due to the availability of more non-zero measurements. However, even at low CR, the reconstruction preserves the essential features of the original image, demonstrating the robustness and effectiveness of the proposed chaotic compressed sensing and reconstruction framework.

TABLE III. COMPARISON WITH EXISTING SYSTEMS

Criteria	Edirisinghe et al. (2024) [25]	Kirichek et al. (2017) [26]	Wei et al. (2021) [27]	Guerra et al. (2023) [28]	Proposed
Technology	ESP32CAM, SX1278	Raspberry Pi Zero, SX1267	Raspberry pi 3B+, SX1276	Raspberry Pi 3B+, SX1272	ESP32CAM, SX1262
Compression Method	JPEG	JPEG/JPEG 2000	WebP with Base64	YCoCg, Wavelet Subbands	Compressed Sensing, Wavelet, TV Minimization
PSNR (dB)	-	23	33.84	21.5 to 27	32.92 (CR = 0.3)
Transmission Time (s)	20	-	25.7	90	30
Security	None	None	None	None	Chaotic Masking

Additionally, Fig. 4 depicts the relationship between MSE and PSNR as the compression ratio (CR) varies. These plot indicates that using more measurements results in a reconstructed image which is closer to the original in terms of pixel-wise accuracy. Conversely, the PSNR increases with higher CR, reflecting improved visual quality of the reconstructed image. It can be consider that, the proposed chaotic compressed sensing and wavelet-TV reconstruction framework achieves a good balance between compression and image quality. Notably, even at moderate compression ratios (CR = 0.4–0.5), the system maintains acceptable reconstruction performance, suggesting suitability for deployment in bandwidth-constrained LoRa-based IoT applications where transmission efficiency is critical.

Table III presents a comparative evaluation between the proposed method and several existing image transmission techniques over LoRa networks. The comparison is based on key parameters such as technology framework, compression method, image quality in terms of PSNR, transmission time, and security features. The proposed system employs the chaotic compressed sensing, wavelet transform, and TV minimization, which enable high efficiency image reconstruction with significantly reduced data volume. Notably, the proposed method achieves a PSNR of 32.92 dB at a compression ratio of 0.3, which is comparable to or better than other approaches, such as the 33.84 dB reported by Wei et al. (2021) using WebP compression, and considerably higher than the 23 dB and 21.5–27 dB reported by Kirichek et al. (2017) and Guerra et al. (2023), respectively. In terms of transmission time, the proposed method achieves a practical 30-second duration, which is faster than the 90 seconds required by Guerra et al., and close to the 25.7 seconds achieved by Wei et al., while also incorporating inherent chaotic masking for data security, unlike all compared works, which offer no security measures. Additionally, while most competing methods rely on image-centric compression formats like JPEG, WebP, or wavelet subbands, the proposed approach achieves compression and encryption simultaneously through chaotic sampling. Overall, this comparison highlights the efficiency, security, and image quality advantages of the proposed method, making it highly suitable for low-power, bandwidth-constrained image transmission in IoT scenarios.

IV. CONCLUSION

This paper presents a hybrid compressed sensing approach tailored for efficient and secure image transmission in LoRa-based IoT systems. The proposed method achieves both sig-

nificant data compression and reliable image reconstruction by integrating a chaotic map-based sensing matrix with wavelet transforms and total variation (TV) minimization. The use of a chaotic sequence not only improves incoherence during the sampling process but also serves as a lightweight encryption mechanism, enhancing data privacy without additional computational overhead. Experimental evaluations on real embedded hardware demonstrate the practical feasibility of the proposed system in low-power environments. The results indicate that even with low compression ratios, the reconstructed images maintain high perceptual quality, with PSNR values exceeding 32 dB. Furthermore, transmission times are reduced to under 30 seconds per image, significantly outperforming traditional JPEG-based and wavelet-subband techniques used in LoRa imaging. A comparative analysis with existing methods highlights the advantages of the proposed approach in terms of image quality, transmission efficiency, power consumption, and embedded security. These benefits make the system particularly well-suited for IoT applications where bandwidth, energy, and processing resources are severely constrained. The proposed system has potential for a wide range of applications, including environmental monitoring, smart agriculture, structural health monitoring, and wildlife surveillance. It can also be applied for remote industrial inspections, where timely visual data from resource-constrained IoT nodes can significantly improve decision-making efficiency and operational safety.

ACKNOWLEDGMENT

The authors are grateful for the collaboration between Temasek Polytechnic and Thai-Nichi Institute of Technology.

REFERENCES

- [1] A. Zanella, N. Bui, A. Castellani, L. Vangelista, and M. Zorzi, "Internet of things for smart cities," *IEEE Internet of Things journal*, vol. 1, no. 1, pp. 22–32, 2014.
- [2] R. Sanchez-Iborra, J. Sanchez-Gomez, J. Ballesta-Viñas, M.-D. Cano, and A. F. Skarmeta, "Performance evaluation of lora considering scenario conditions," *Sensors*, vol. 18, no. 3, 2018. [Online]. Available: <https://www.mdpi.com/1424-8220/18/3/772>
- [3] M. J. Faber, K. M. van der Zwaag, W. G. V. dos Santos, H. R. d. O. Rocha, M. E. V. Segatto, and J. A. L. Silva, "A theoretical and experimental evaluation on the performance of lora technology," *IEEE Sensors Journal*, vol. 20, no. 16, pp. 9480–9489, 2020.
- [4] A. H. Jebri, A. Sali, A. Ismail, and M. F. A. Rasid, "Overcoming limitations of lora physical layer in image transmission," *Sensors*, vol. 18, no. 10, 2018. [Online]. Available: <https://www.mdpi.com/1424-8220/18/10/3257>

- [5] J. Kim, M. Kwak *et al.*, "Reliable image transmission over lora networks." *Issues in Information Systems*, vol. 25, no. 1, 2024.
- [6] S. Li, H. Song, and M. Iqbal, "Privacy and security for resource-constrained iot devices and networks: Research challenges and opportunities," *Sensors*, vol. 19, no. 8, 2019. [Online]. Available: <https://www.mdpi.com/1424-8220/19/8/1935>
- [7] S. Kumar, D. Kumar, R. Dangi, G. Choudhary, N. Dragoni, and I. You, "A review of lightweight security and privacy for resource-constrained iot devices," *Computers, Materials and Continua*, vol. 78, no. 1, pp. 31–63, 2024.
- [8] A. Shafique, A. Mehmood, M. Alawida, and A. N. Khan, "Enhancing privacy in data transmission between iot devices: A robust encryption and embedding framework for secure and meaningful image communication," *Journal of Information Security and Applications*, vol. 93, p. 104112, 2025. [Online]. Available: <https://www.sciencedirect.com/science/article/pii/S2214212625001498>
- [9] P. Hu, J. Im, Z. Asgar, and S. Katti, "Starfish: Resilient image compression for aiot cameras," in *Proceedings of the 18th Conference on Embedded Networked Sensor Systems*, 2020, pp. 395–408.
- [10] P. Chakraborty, J. Cruz, and S. Bhunia, "Leveraging domain knowledge using machine learning for image compression in internet-of-things," *arXiv preprint arXiv:2009.06742*, 2020.
- [11] A. Hojjat, J. Haberer, and O. Landsiedel, "McuCoder: Adaptive bitrate learned video compression for iot devices," 2024. [Online]. Available: <https://arxiv.org/abs/2411.19442>
- [12] Y. Shuling, Y. Renping, and W. Longzhi, "Transmission line monitoring technology based on compressed sensing wireless sensor network," *International Journal of Advanced Computer Science & Applications*, vol. 15, no. 4, 2024.
- [13] H. Djelouat, A. Amira, and F. Bensaali, "Compressive sensing-based iot applications: A review," *Journal of Sensor and Actuator Networks*, vol. 7, no. 4, 2018. [Online]. Available: <https://www.mdpi.com/2224-2708/7/4/45>
- [14] Z. Wang, S. Sun, Y. Li, Z. Yue, and Y. Ding, "Distributed compressive sensing for wireless signal transmission in structural health monitoring: An adaptive hierarchical bayesian model-based approach," *Sensors*, vol. 23, no. 12, 2023. [Online]. Available: <https://www.mdpi.com/1424-8220/23/12/5661>
- [15] M. F. Duarte, M. A. Davenport, D. Takhar, J. N. Laska, T. Sun, K. F. Kelly, and R. G. Baraniuk, "Single-pixel imaging via compressive sampling," *IEEE signal processing magazine*, vol. 25, no. 2, pp. 83–91, 2008.
- [16] M. Lustig, D. Donoho, and J. M. Pauly, "Sparse mri: The application of compressed sensing for rapid mr imaging," *Magnetic Resonance in Medicine: An Official Journal of the International Society for Magnetic Resonance in Medicine*, vol. 58, no. 6, pp. 1182–1195, 2007.
- [17] F. Chaparro B., M. Pérez, and D. Mendez, "A communication framework for image transmission through lpwan technology," *Electronics*, vol. 11, no. 11, 2022. [Online]. Available: <https://www.mdpi.com/2079-9292/11/11/1764>
- [18] L. R. Chandran, I. Karuppasamy, M. G. Nair, H. Sun, and P. K. Krishnakumari, "Compressive sensing in power engineering: A comprehensive survey of theory and applications, and a case study," *Journal of Sensor and Actuator Networks*, vol. 14, no. 2, 2025. [Online]. Available: <https://www.mdpi.com/2224-2708/14/2/28>
- [19] M. S. Khan, A. Al-Dubai, J. Ahmad, N. Pitropakis, and B. Ghaleb, "A novel feature-aware chaotic image encryption scheme for data security and privacy in iot and edge networks," 2025. [Online]. Available: <https://arxiv.org/abs/2505.00593>
- [20] E. Setyaningsih and R. Wardoyo, "Review of image compression and encryption techniques," *International Journal of Advanced Computer Science and Applications*, vol. 8, no. 2, 2017. [Online]. Available: <http://dx.doi.org/10.14569/IJACSA.2017.080212>
- [21] L. Gong, K. Qiu, C. Deng, and N. Zhou, "An image compression and encryption algorithm based on chaotic system and compressive sensing," *Optics & Laser Technology*, vol. 115, pp. 257–267, 2019. [Online]. Available: <https://www.sciencedirect.com/science/article/pii/S0030399218304961>
- [22] L. Li, Y. Fang, L. Liu, H. Peng, J. Kurths, and Y. Yang, "Overview of compressed sensing: Sensing model, reconstruction algorithm, and its applications," *Applied Sciences*, vol. 10, no. 17, 2020. [Online]. Available: <https://www.mdpi.com/2076-3417/10/17/5909>
- [23] W. San-Um and P. Ketthong, "The generalization of mathematically simple and robust chaotic maps with absolute value nonlinearity," in *TENCON 2014 - 2014 IEEE Region 10 Conference*, 2014, pp. 1–4.
- [24] W. San-Um, P. Ketthong, W. Chankasame, and J. Noymanee, "A cost-effective true random bit generator using a pair of robust signum-based chaotic maps," in *2015 Science and Information Conference (SAI)*, 2015, pp. 1305–1310.
- [25] S. Edirisinghe and Sachinda, "Image transmission using lora for edge learning," *SSRN Electronic Journal*, 02 2024.
- [26] R. Kirichek, V.-D. Pham, A. Kolechkin, M. Al-Bahri, and A. Paramonov, "Transfer of multimedia data via lora," in *Internet of Things, Smart Spaces, and Next Generation Networks and Systems*, O. Galinina, S. Andreev, S. Balandin, and Y. Koucheryavy, Eds. Cham: Springer International Publishing, 2017, pp. 708–720.
- [27] C.-C. Wei, P.-Y. Su, C.-C. Chang, and K.-C. Chang, "A study on lora dynamic image transmission," in *2021 IEEE 4th International Conference on Knowledge Innovation and Invention (ICKII)*, 2021, pp. 10–13.
- [28] K. Guerra, J. Casavilca, S. Huamán, L. López, A. Sanchez, and G. Kemper, "A low-rate encoder for image transmission using lora communication modules," *International Journal of Information Technology*, vol. 15, no. 2, pp. 1069–1079, Feb 2023. [Online]. Available: <https://doi.org/10.1007/s41870-022-01077-7>